

13

4

An Investigation of the Structure of the Hydrated Electron based on Unpaired  
Electron Densities Calculated by the INDO Method<sup>1</sup>

by Carolyn M. L. Kerr<sup>\*2</sup> and Ffrancon Williams

Department of Chemistry, University of Tennessee, Knoxville, Tennessee 37916

(Received

)

Publication costs assisted by the U.S. Atomic Energy Commission

Spin density distributions have been calculated for a number of possible structures for the hydrated electron, and the total spin density associated with the hydrogen atoms compared with the value derived from esr experiments. Although the agreement with experiment is not close, the best results are obtained for a planar dimeric structure containing two central hydrogens close to one another. The structure of the hydrated electron may incorporate symmetrically placed units of this type. ..

Editorial correspondence and proofs should be sent to:

Ffrancon Williams  
Department of Chemistry  
University of Tennessee  
Knoxville, Tennessee 37916

## 1. Introduction

In this study the INDO method<sup>3</sup> has been employed to investigate the structure of the hydrated electron using a comparison of the experimental and theoretical spin densities on the hydrogen nuclei as a criterion of structural validity. This approach is used in preference to the conventional one of minimizing the energy of the system with respect to geometrical parameters for two reasons. First, the spin density distribution for a paramagnetic species is generally very sensitive to the molecular structure, and the INDO method has been shown to yield isotropic hyperfine coupling constants in good agreement with experiment for a wide variety of both  $\sigma$  and  $\pi$  radicals whose geometries can be reasonably well defined.<sup>3c</sup> The agreement is generally better for hydrogen than for second row elements. Secondly, the INDO method is not always reliable for predicting equilibrium geometries based on energy minimization. This is hardly surprising since the parameterization was intended to yield charge densities and spin densities rather than properties dependent on the molecular energies.<sup>4</sup>

The use of a completely molecular description instead of the familiar cavity or polaron models<sup>5</sup> of the hydrated electron stems from recent work in this laboratory on electron excess centers in acetonitrile<sup>6</sup> and sulfuric chloride.<sup>7</sup> In acetonitrile,  $\gamma$ -irradiation yields either the monomer or dimer radical anion depending upon the crystalline phase. The monomer radical anion is a typical  $\sigma$ -radical with appreciable spin density in the 2s orbital of the nitrile carbon due to the bending of the molecule. On

the other hand, the spin density distribution in the dimer radical anion indicates the unpaired electron is associated with two equivalent and essentially linear molecules, with most of the spin density in the p orbitals on nitrogen. According to a simple MO description, the dimer radical anion can be considered as a radical anion complex in which the unpaired electron occupies a supramolecular bonding orbital derived from the antibonding orbitals of two separate molecules. The radical anion of sulfuryl chloride can be described similarly, and in this case the molecular orbitals involved are essentially the lowest antibonding orbitals of adjacent sulfur dioxide and chlorine molecules.

In certain respects, the properties of the dimer radical anion of acetonitrile resemble those of trapped electrons in glasses. In particular, the esr signals of both these species saturate readily with microwave power and the optical absorption spectra are characteristically broad. These similarities suggest that in the case of trapped or solvated electrons, the excess electron may be confined to the orbitals of two or more solvent molecules rather than to an interstitial cavity. According, the hydrated electron can be formally represented as  $(\text{H}_2\text{O})_{\underline{n}}^{\cdot-}$ .

The esr spectrum of the trapped electron in aqueous solids is generally a broad singlet but hyperfine structure has been resolved in two instances.<sup>8,9</sup> Both in crystalline ice co-deposited with alkali metals<sup>8</sup> and, more recently, in a  $\gamma$ -irradiated alkaline glass,<sup>9</sup> the spectrum was shown to consist of an odd multiplet with a splitting of approximately 5 G. From these results, it has been suggested that the trapped electron interacts with either

four<sup>8</sup> or six<sup>9</sup> protons. In any event, the existence of resolved hyperfine features certainly points to a well-defined molecular structure for  $(\text{H}_2\text{O})_{\underline{n}}^{\cdot-}$  rather than to a disordered cage of water molecules surrounding a trapped electron. A lineshape analysis<sup>10</sup> on the unresolved spectrum also indicates that the hyperfine interaction is limited to a relatively small number ( $8 \pm 2$ ) of protons. If eight protons can be considered an upper limit, the observed hfs of 5 G as compared to the value of ca. 500 G for the isolated H<sup>•</sup> atom indicates a spin density of ca. 1% and hence a total for the complex of 8% or less. The aim of the present work has been to seek structures of  $(\text{H}_2\text{O})_{\underline{n}}^{\cdot-}$  for which the calculated spin density distribution approximates most closely to this experimental result.

## 2. Calculations

The INDO method employs a valence orbital basis set which in this case consists of the 1s orbitals on hydrogen and 2s and 2p orbitals on oxygen. The calculations yield the spin density distribution of the excess electron over the valence shell orbitals of the water molecules in the complex.

Bond orders between two atoms were calculated as the sum of all off-diagonal elements involving the atoms in the charge density matrix. While the numerical values obtained have no absolute significance, comparison of bond orders in a closed shell species and in the negatively charged open shell species with the same geometry can be used to determine the bond-breaking or bond-forming effect resulting from the addition of an electron.

### 3. Results

The results of calculations on the monomer,  $\text{H}_2\text{O}^-$ , are presented first. For this species, the OH bond length was varied from 0.08 to 0.19 nm in increments of 0.01 nm, and the HOH angle from  $60^\circ$  to  $180^\circ$  in increments of  $10^\circ$ . The corresponding values for the neutral molecule are 0.096 nm and  $105^\circ$ .<sup>11</sup> Positive spin density is always obtained in the s orbitals of both hydrogen and oxygen. There is also considerable spin density in the oxygen  $p_x$  and  $p_y$  orbitals, but none in the  $p_z$  orbital (see Figure 1 (a)). The spin densities in the  $p_x$  and  $p_y$  orbitals are always of opposite sign, and increase monotonically with the bond length. The positive spin density is associated with the  $p_y$  orbital for OH distances of 0.08 - 0.14 nm and for HOH angles of  $60-90^\circ$ , and with the  $p_x$  orbital for all other geometries. The total spin density on hydrogen,  $\rho_H^T$ , where this quantity is defined generally for multimeric species as

$$\rho_H^T = \sum_{\text{all H}} |\rho_H| ,$$

varies both with bond angle and bond length as shown in Figure 2. For the shorter bond lengths, minima occur in the curves for angles of  $100$  to  $110^\circ$ , but there is no corresponding optimum bond length,  $\rho_H^T$  increasing regularly as the OH distance is increased. The O-H bond order decreases steadily with increasing bond length, and for bond lengths up to 0.14 nm, it has a value which is about 0.7 times that of the neutral molecule

with the same geometry. For higher bond lengths, the bond orders for  $\text{H}_2\text{O}^-$  and  $\text{H}_2\text{O}$  are both small. These factors and the high negative spin densities observed in the oxygen p orbitals suggest that the large values of  $\rho_{\text{H}}^{\text{T}}$  and their variation with bond length reflect a progressive breakdown in the OH bonding.

The large  $\rho_{\text{H}}^{\text{T}}$  found for  $\text{H}_2\text{O}^-$  definitely excludes this as the structure of the hydrated electron. However, by analogy with acetonitrile where there are profound differences between the spin density distributions and structures of monomer and dimer radical anion, this does not rule out the possibility that suitable combinations of  $\text{H}_2\text{O}$  molecules could yield values of  $\rho_{\text{H}}^{\text{T}}$  in closer accord with experiment. Based on this, our approach has involved the determination of  $\rho_{\text{H}}^{\text{T}}$  for multimeric species  $(\text{H}_2\text{O})_{\underline{n}}^-$ . Since the values of  $\rho_{\text{H}}^{\text{T}}$  for the monomer are extremely large, we have investigated various geometrical arrangements of molecules in  $(\text{H}_2\text{O})_{\underline{n}}^-$  complexes to determine which configurations lead to a decrease in  $\rho_{\text{H}}^{\text{T}}$ .

Calculations have been done on a variety of different dimeric structures. The first set of structures are shown in Figure 1, (b)-(f). The distinguishing feature of these is that the oxygen p orbitals are aligned so that a strong overlap is possible. It has been shown previously<sup>7</sup> that an excess electron can be effectively shared between two molecules through positive overlap of antibonding orbitals from the separate molecules. An additional consideration in the present case is that bonding between the  $\text{H}_2\text{O}$  molecules through the oxygen p orbitals might redistribute the spin density in favor of these orbitals, thereby decreasing  $\rho_{\text{H}}^{\text{T}}$ .

For any particular structure, equivalent  $\text{H}_2\text{O}$  geometries were always employed. The OH bond length, the HOH angle, and  $\underline{d}$ , the distance apart of the oxygen atoms, were varied independently over the ranges 0.09 - 0.12 nm,  $90 - 135^\circ$ , and 0.16 - 0.24 nm, respectively. The results showed that in structure (b), there appeared to be no delocalization and the distribution was essentially that of the  $\text{H}_2\text{O}^-$  monomer and a neutral  $\text{H}_2\text{O}$  molecule for all configurations; in all the other structures, the unpaired electron was shared equally between the two molecules. For structures (c) and (d), there was no reduction in  $\rho_{\text{H}}^{\text{T}}$  whereas a reduction was found for structures (e) and (f), this being larger in the case of the former for all configurations. A number of structures intermediate between (e) and (f) were generated by allowing the hydrogen atoms of the upper molecule to range over the surface of a hemisphere, as shown in Figure 1(e). For all of these,  $\rho_{\text{H}}^{\text{T}}$  was found to be greater than the value for structure (e), suggesting that parallel alignment of the p orbitals is a contributing factor in reducing  $\rho_{\text{H}}^{\text{T}}$ .

The calculations were extended to trimer and tetramer for model (e). Although there were some irregularities, in general  $\rho_{\text{H}}^{\text{T}}$  decreased monotonically in going from monomer to tetramer and the largest decreases were observed for OH bond lengths of 0.11 - 0.12 nm, an HOH angle of  $105^\circ$ , and  $\underline{d} = 0.18 - 0.20$  nm. The results are summarized in Table I. For these geometries, the spin density on oxygen is largely in the  $p_{\underline{x}}$  orbital with small negative contributions in the  $p_{\underline{y}}$  and  $p_{\underline{z}}$  orbitals, as shown in

Table II. It can also be seen from the data given in this Table that the overall distribution of the spin density in an individual molecule is not greatly altered between monomer and tetramer.

The models discussed above are somewhat unrealistic. Since the microstructure of an aqueous solid is controlled by hydrogen bonding, models in which molecules are linked by hydrogen bonding should also be considered. Although other configurations have been observed, hydrogen bonded systems generally involve linear or nearly linear O-----H---O units. A simple dimer incorporating this feature is shown in Figure 3(a), the O-----H---O line making an approximately tetrahedral angle with the O-H bonds of molecule 2. Calculations were performed for the same range of bond lengths and bond angles as previously and oxygen-oxygen distances of 0.24 to 0.30 nm (the corresponding distance in ice is 0.276 nm<sup>11</sup>). In all these cases, the unpaired electron was effectively localized on one molecule. Small rotations (up to 30°) of molecule 2 about the three coordinate axes (see Figure 1(a)) hardly affected the delocalization or the value of  $\rho_H^T$ , indicating that structures derived from a hydrogen-bonded fragment are unfavorable.

Further calculations were then carried out for an OH bond length of 0.11 nm, an HOH bond angle of 105°, an oxygen-oxygen distance of 0.27 nm, and configurations such that the position of molecule 1 and the linearity of the O-----H---O unit were retained and the hydrogen



atoms of molecule 2 were rotated over the surface of a sphere. Over a small range of configurations, both delocalization and a decrease in  $\rho_H^T$  were observed. Once the configuration yielding the minimum value of  $\rho_H^T$  had been determined,  $\rho_H^T$  was minimized with respect to the bond length, bond angle, and oxygen-oxygen distance, these parameters being varied over the ranges 0.09 to 0.12 nm, 90 to 135°, and 0.23 to 0.35 nm, respectively. The lowest value of  $\rho_H^T$  was found for the configuration shown in Figure 3 (b) with an OH bond length of 0.12 nm, a bond angle of 105°, and an oxygen-oxygen distance of 0.31 nm. The spin density distributions for this structure and for the monomer with the same molecular geometry are shown in Table III. A further limited number of calculations were performed with the above molecular geometry, but varying the orientations of both molecules and the distance between them. Spin densities close to the values obtained for the dimer in Figure 3(b) were found for dimers symmetrical about the oxygen-oxygen axis and with hydrogen-hydrogen distances of 0.08 to 0.09 nm. Slightly higher spin densities were obtained for symmetrical dimers containing linear  $O-H\cdots H-O$  units. The minimum values of  $\rho_H^T$  found for these structures are listed (Table III) with the associated structural parameters and spin densities.

From the data given in Table III, it can be seen that the distribution is substantially different for monomer and dimer, in contrast to the results obtained for model (c). There is a marked shift of both spin density and charge density from hydrogen to oxygen in the dimer relative to the monomer. A further point to note is that the spin densities in all orbitals of the dimers in Table III are zero or positive.

The proximity of the central hydrogen atoms appears to be an important feature of these structures. Low values of  $\rho_{\text{H}}^{\text{T}}$  were only observed for hydrogen-hydrogen distances in the range 0.07 - 0.10 nm, and these were associated with bond orders between the hydrogen atoms of 0.5 - 0.7. The bond orders in the corresponding neutral molecule dimer are almost a factor of two less than this, and the values for isolated hydrogen molecules are 1.0.

#### 4. Discussion

In this paper we have examined the possibilities for determining the structure of the hydrated electron by comparison of theoretical and experimental unpaired electron densities. Although the investigations of the various structures are not exhaustive, they are reasonably detailed and lead to two general conclusions. Firstly, dimers with certain configurations can yield values of  $\rho_{\text{H}}^{\text{T}}$  substantially less than that for the monomer with the same molecular geometry. Secondly, for a dimer structure which was shown to yield a reduced  $\rho_{\text{H}}^{\text{T}}$ , then further reduction was obtained by increasing the number of molecules in the complex.

It is interesting that the optimum dimer model on the basis of spin densities is structurally similar to others proposed on other grounds. The dimer structure suggested by Raff and Pohl<sup>12</sup> consists essentially of an  $\text{H}_2^+$  fragment perturbed by two  $\text{OH}^-$  ions. A degree of bonding is thus implied between the central hydrogens. This model yields a value for the optical excitation energy in good agreement with experiment. Webster and

his co-workers<sup>13</sup> have investigated a similar model, viz. a planar dimer containing a linear O—H-----H—O unit, using two different molecular orbital methods. In both cases, structures corresponding to the minimum energy give excitation energies close to the experimental value. However, the predicted hydrogen-hydrogen separations (0.12 nm for the INDO and 0.15 nm for the extended Hückel method) are somewhat larger than the range (0.07-0.10 nm) found in the present work.

While the dimer shown in Figure 3(b) clearly does not represent the complete structure of the hydrated electron, it has several favorable features which suggest that the complete structure may incorporate units of this type. Moreover, if a larger even number of molecules, i.e. four or six, is used, symmetrical structures can be constructed which contain four or more equivalent protons as required by the esr results,<sup>8-10</sup> and calculations are currently in progress for these systems.

—  
Acknowledgment. We would like to thank Dr. J. E. Bloor for his help and advice, and for lending us his INDO program.

## REFERENCES

- (1) This research was supported by the U.S. Atomic Energy Commission under Contract No. AT-(40-1)-2968, and this is AEC Document No. ORO-2968-75.
- (2) Author to whom correspondence should be addressed at the Department of Chemistry, The University, Southampton, SO9 5NH, Hampshire, England.
- (3) (a) J. A. Pople and D. L. Beveridge, "Approximate Molecular Orbital Theory," McGraw-Hill Book Co., New York, N.Y., 1970; (b) Program 141, Quantum Chemistry Program Exchange, Department of Chemistry, Indiana University, Bloomington, Ind. 47401. Computations were carried out on an IBM System 360/65 digital computer; (c) J. A. Pople, D. L. Beveridge, and P. A. Dobosh, J. Amer. Chem. Soc., 90, 4201 (1968).
- (4) J. N. Murrell and A. J. Harget, "Semi-empirical SCF Molecular Orbital Theory of Molecules," Wiley-Interscience, New York, N.Y., 1972, p 57.
- (5) J. Jortner in "Actions Chimiques et Biologiques des Radiations," M. Haissinsky, Ed., Volume 14, Masson et Cie., Paris, 1970.
- (6) E. D. Sprague, K. Takeda, and F. Williams, Chem. Phys. Lett., 10, 299 (1971).
- (7) (a) C. M. L. Kerr and F. Williams, J. Amer. Chem. Soc., 93, 2805 (1971); (b) C. M. L. Kerr and F. Williams, ibid., 94, 0000 (1972).
- (8) J. E. Bennett, B. Mile, and A. Thomas, J. Chem. Soc., A, 1393 (1967); J. E. Bennett, B. Mile, and A. Thomas, ibid., 1502 (1969).
- (9) K. Ohno, I. Takemura, and J. Sohma, J. Chem. Phys., 56, 1202 (1972).
- (10) B. G. Ershov and A. K. Pikaev, Radiation Res. Rev., 2, 1 (1969).
- (11) L. Pauling, "The Nature of the Chemical Bond," 3rd ed, Cornell University Press, Ithaca, N.Y., 1960, pp 110, 464.
- (12) L. Raff and H. A. Pohl, Adv. Chem. Ser., 50, 173 (1965).
- (13) (a) B. J. McAloon and B. C. Webster, Theor. Chim. Acta, 15, 385 (1969); (b) G. Howat and B. C. Webster, Ber. Bunsenges. Phys. Chem., 75, 626 (1971).

## FIGURE CAPTIONS

Figure 1. Models used in INDO calculations on the structure of the hydrated electron: (a) monomer shown with the coordinate axis system which defines the directions of the oxygen p orbitals for all models in this Figure and in Figure 3; (b) -(f) represent various dimer models incorporating aligned oxygen p orbitals of the individual molecules.

Figure 2. Variation of  $\rho_H^T$  for  $H_2O^-$  with the HOH angle for various OH bond lengths. Bond lengths are given in nm.

Figure 3. (a) A dimer model for the hydrated electron incorporating hydrogen bonding; (b) dimer model found to give lowest value of  $\rho_H^T$ . This model is planar with an OH bond length of 0.12 nm, an HOH angle of  $105^\circ$ , an oxygen-oxygen distance of 0.31 nm, and a distance between central hydrogens of 0.072 nm.

Table I: Values of  $\rho_H^T$  for Model (e) Multimers<sup>a</sup>

OH bond length nm	HOH angle degrees	O-O distance nm	$\rho_H^T$				$\rho_H^T$ (tetramer)
			monomer	dimer	trimer	tetramer	$\rho_H^T$ (monomer)
0.11	105	0.18	0.644	0.533	0.480	0.443	0.69
0.11	105	0.20	0.644	0.537	0.519	0.448	0.70
0.12	105	0.18	0.706	0.537	0.463	0.383	0.54

<sup>a</sup>These geometries yielded minimum values of  $\rho_H^T$  for the tetramer.

Table II: Comparison of Spin Density Distributions for Monomers and Model (e) Tetramers with the Same Molecular Geometry<sup>a</sup>

OH bond length nm	HOH angle degrees	O-O distance nm	Species		<sup>b</sup> $\rho_H$	$\rho_O^s$	$\rho_O^{p_x}$	$\rho_O^{p_y}$	$\rho_O^{p_z}$
0.11	105	----	monomer <sup>c</sup>		0.322	0.107	0.377	0.000	-0.128
0.11	105	0.18	tetramer <sup>d</sup>	(1,4)	0.015	0.015	0.055	-0.003	-0.005
				(2,3)	0.096	0.055	0.203	-0.008	-0.033
				total	0.222	0.140	0.516	-0.022	-0.076
0.11	105	0.18	tetramer <sup>d</sup>	(1,4)	0.012	0.010	0.050	-0.001	-0.004
				(2,3)	0.101	0.052	0.207	-0.003	-0.036
				total	0.226	0.124	0.514	-0.008	-0.080
0.12	105	----	monomer <sup>c</sup>		0.352	0.085	0.397	0.000	-0.185
0.12	105	0.20	tetramer <sup>d</sup>	(1,4)	0.003	0.007	0.064	-0.001	-0.001
				(2,3)	0.093	0.040	0.246	-0.004	-0.044
				total	0.192	0.094	0.620	-0.010	-0.090

<sup>a</sup>These geometries yielded minimum values of  $\rho_H^T$  for the tetramers. <sup>b</sup>Refers to only one hydrogen nucleus. In all molecules the hydrogens are equivalent. <sup>c</sup>The monomer is considered to be in the xz plane as are the individual molecules of the tetramer (see Figure 1). <sup>d</sup>The molecules in the tetramer are equivalent in pairs.

Table III: Comparison of Spin Density Distributions for Monomer and Dimer Species Yielding Minimum  $\rho_H^T$  Values

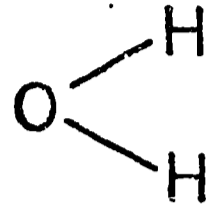
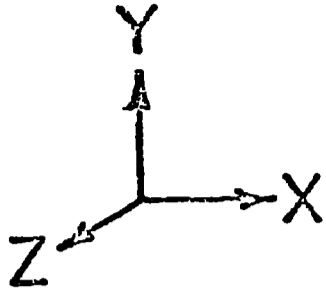
Species <sup>a</sup>	O-O distance nm	H-H distance nm	$\rho_H$ outer	$\rho_H$ inner	$\rho_O^s$	$\rho_O^{px}$	$\rho_O^{py}$	$\rho_O^{pz}$	$\rho_H^T$
monomer	----	----	0.352	0.352	0.085	0.397	-0.185	0.000	0.704
dimer (as in Fig. 3(b))	0.31	0.072	0.012 0.013	0.105 0.079	0.045 0.040	0.021 0.071	0.360 0.256	0.000 0.000	0.208
symmetrical dimer <sup>b,c</sup>	0.31	0.079	0.012	0.092	0.043	0.043	0.310	0.000	0.208
linear dimer <sup>b,d</sup>	0.33	0.090	0.018	0.091	0.041	0.064	0.287	0.000	0.217

<sup>a</sup>The molecular geometry is the same for all these species (OH bond distance = 0.12 nm, HOH angle = 105°).

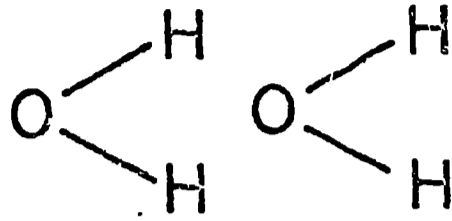
<sup>b</sup>The molecules are equivalent. The total spin density associated with any type of orbital is thus twice the quoted value. <sup>c</sup>Planar configuration as in Fig. 3(b) except that the molecules have both been rotated until

the center hydrogens are symmetrically placed with respect to the oxygen-oxygen axis. <sup>d</sup>Planar configuration as in Fig. 3(b) except that molecule 2 has been rotated until both inner hydrogens are linear with the oxygens.

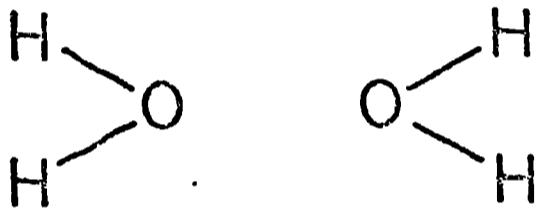




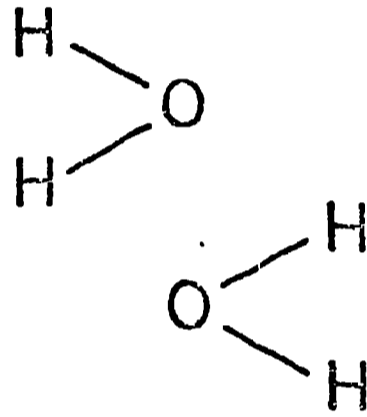
(a)



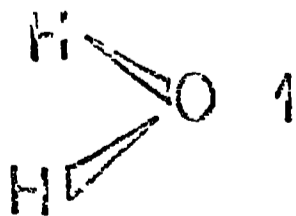
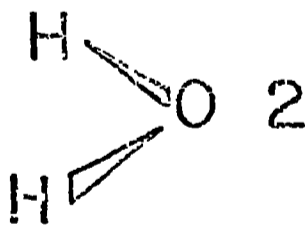
(b)



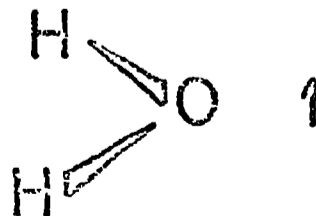
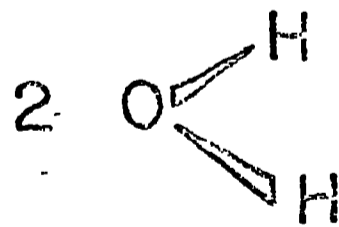
(c)



(d)



(e)



(f)

Figure 1 Kerr and Williams

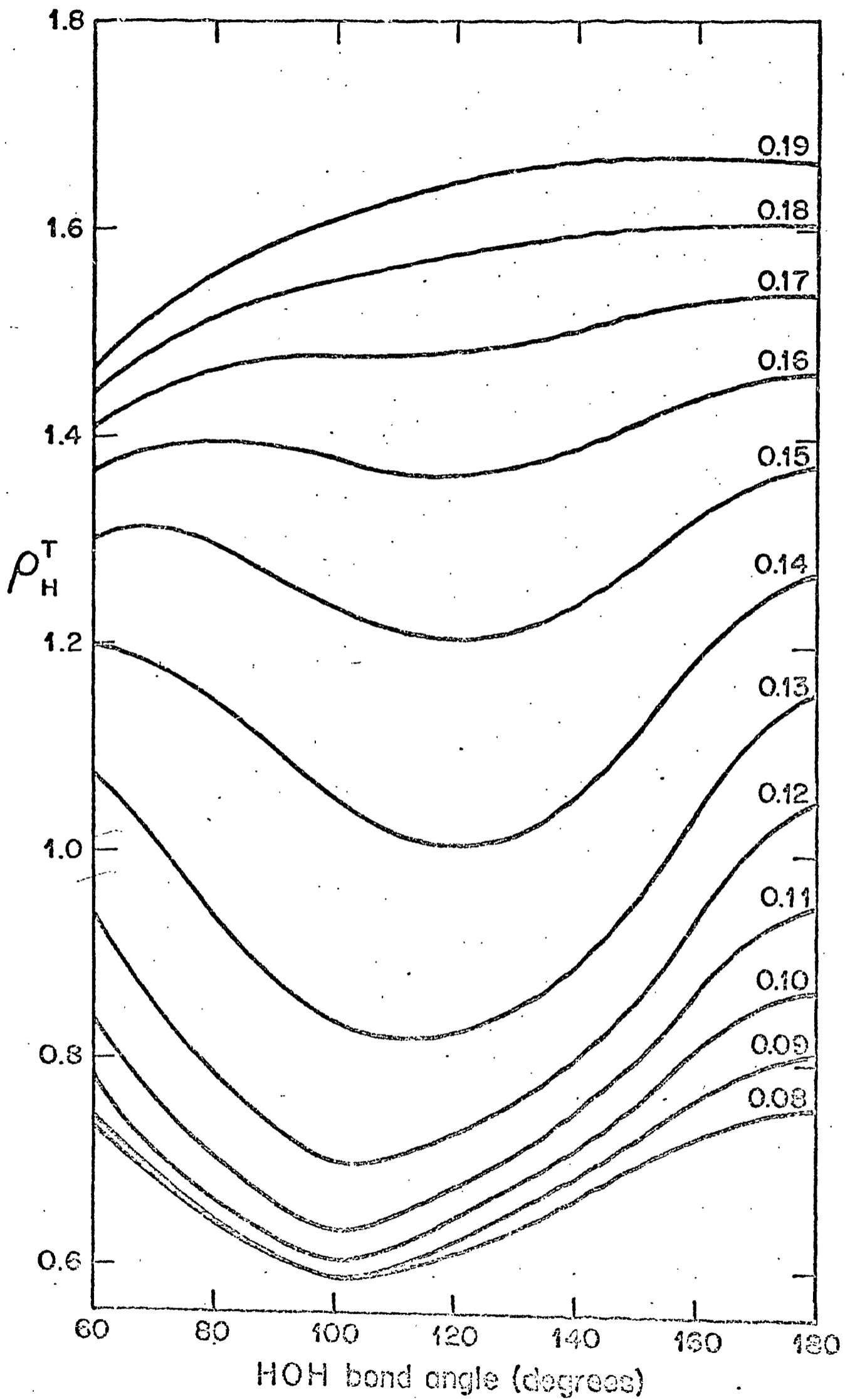


Figure 2 Kerr and Williams

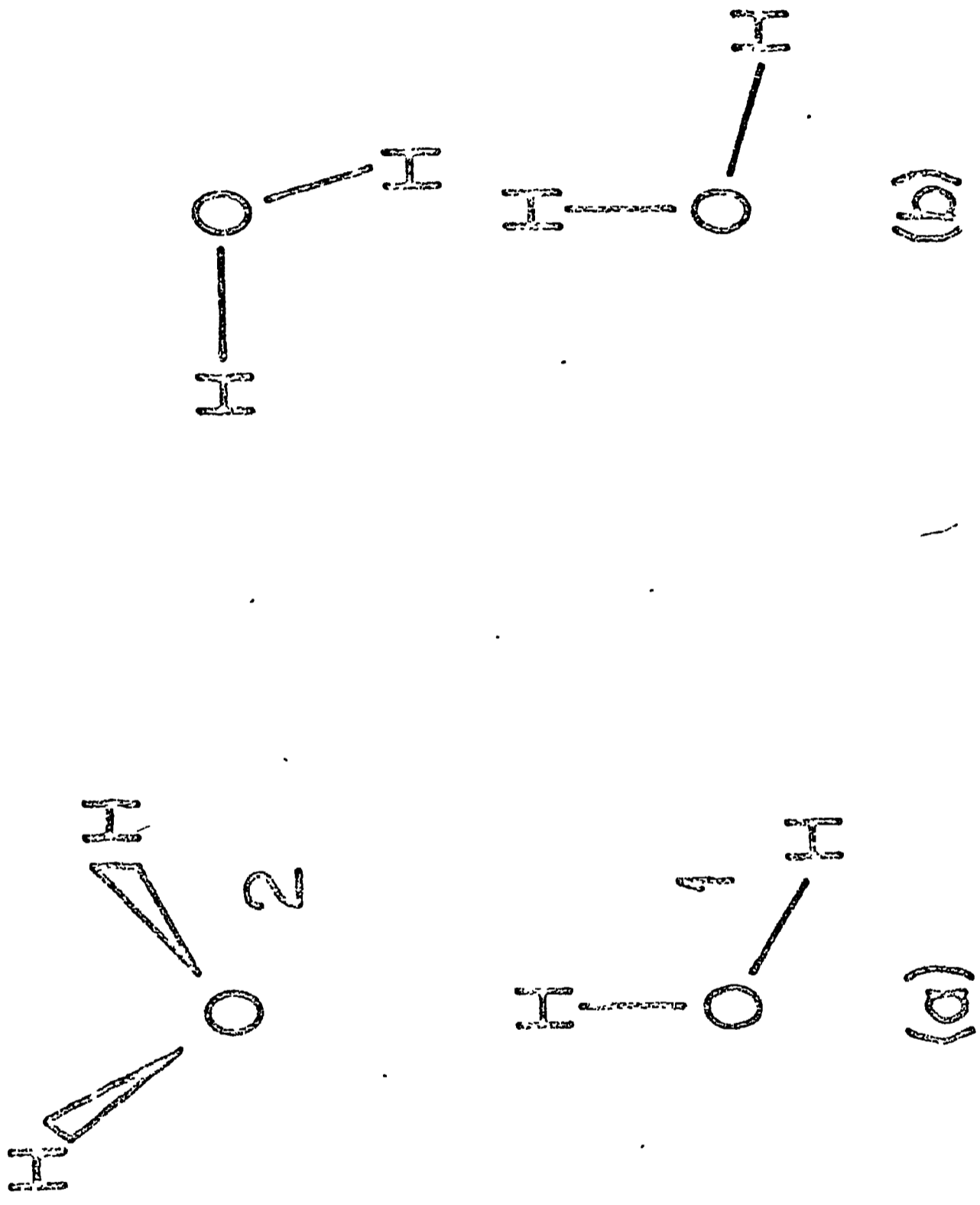


Figure 3 Kerr and Williams